The H.E.S.S. Standard Analysis Technique

Wystan Benbow for the H.E.S.S. Collaboration
Max Planck Institut für Kernphysik
Postfach 103980
D-69029 Heidelberg, Germany

The High Energy Stereoscopic System (H.E.S.S) is an array of four imaging atmospheric-Cherenkov telescopes located in Namibia. With the ability to detect a 1% Crab Nebula flux source in $\sim$25 hours of observation, H.E.S.S. is currently the most sensitive detector of astrophysical VHE ($>$100 GeV) photons. The H.E.S.S. collaboration has published the detection of more than 30 sources of VHE γ-ray emission. The standard analysis technique used in these publications for reconstructing the direction and energy of incident γ-rays, rejecting the large cosmic-ray background, and determining the spectrum and flux of the detected sources is presented.

1 Introduction

Due to the limited size of satellite observatories, a ground-based detector is required for VHE γ-ray astronomy. However, the atmosphere is opaque to VHE photons, so the secondary effects of the atmospheric absorption of these photons must be detected. The H.E.S.S. experiment (see [1] for more details) detects the flashes of Cherenkov light emitted from the electromagnetic cascade of secondary particles, known as an extensive air shower (EAS), resulting from the initial interaction of the γ-ray primary. Astronomical observations are possible since an EAS and its Cherenkov light pool retain the original direction of the incident photon to a high degree. An accurate determination of the primary photon's energy can also be made since the number of Cherenkov photons generated by an EAS is strongly correlated with this energy. Unfortunately, γ-ray observations are severely limited by charged cosmic-ray particles which are $\sim$10,000 times more numerous than a photon of a given energy, and which produce superficially similar EAS. However, subtle differences between the cascades initiated by photons and hadronic particles can be exploited to reject almost all of the cosmic-ray background. This contribution details the techniques employed by H.E.S.S. to determine the energy and direction of VHE γ-rays, to reject most of the hadronic background, and to measure the flux and energy spectrum of any detected

γ-rays. While there are other independent techniques used by H.E.S.S. [2, 3], this text refers to the *Standard Analysis* which appears in essentially all of the H.E.S.S. publications to date.

2 The H.E.S.S. Standard Analysis

H.E.S.S observations are generally taken in 28 minute runs using a central trigger system [4] that requires a minimum of two telescopes be triggered by the Cherenkov light from an EAS. This enables H.E.S.S. to use stereoscopic event-reconstruction techniques and reject almost all images from local muons[1] at the hardware level. Before analysis, every H.E.S.S. run must first pass conservative selection criteria which remove runs affected by hardware malfunctions or poor observing conditions. Images from the data passing the run selection criteria are then calibrated [5] and "cleaned" to remove noise from the image. The image cleaning is done using a two-stage tail-cut procedure which requires a pixel to have a signal greater than 10 (or 5) photoelectrons (PEs) and a neighboring pixel to have a signal larger than 5 (or 10) PEs. After this image cleaning is performed, the moments (e.g. width and length) of the elliptical shower image are parameterized using a Hillas-type analysis [6]. The results of this parameterization are the basis of all the *Standard Analysis* techniques. Only images which exceed a minimum total signal and which pass a distance cut requiring the image center of gravity to be less than 2° from the center of the camera are used in the reconstruction. The size cut (minimum total signal) ensures that the images are well reconstructed and the distance cut eliminates images truncated by the edge of the camera. A minimum of two telescopes passing both the size and distance cuts are required for event reconstruction.

2.1 Geometrical Reconstruction

The shower geometry (i.e. incident direction of the primary particle and shower core location) of each event is reconstructed using techniques pioneered by the HEGRA collaboration. A modified version of Algorithm 1 from [7] is employed. Here, the major axis of each elliptical image is used. The shower direction is determined from a weighted average of the intersections of all pairs of major axes projected in the field of view. The weights incorporate the sine of the angle between the two axes, the size of the two images, and the ratio of width/length from each image. The shower core location is similarly determined using the intersections of the shower axes relative to each telescope position, projected in the plane perpendicular to the respective telescope's pointing direction. The typical angular resolution is $\sim 0.1^\circ$ per event, and the

[1] These images can comprise a significant fraction of a single telescope event rate.

average accuracy in the determination of the shower core location is $\sim$10 m. The small point spread function is comparable to that of the ASCA X-ray satellite, and when combined with the large (5°) field of view and small pointing error (<20" in each direction) of H.E.S.S., allows the morphology of extended VHE γ-ray sources to be resolved as well as enabling sensitive surveys of the VHE sky.

2.2 Background Rejection

The much more numerous cosmic-ray background events are rejected by exploiting the fact that images of a hadron-initiated EAS are on average longer and wider than those initiated by γ-rays. Cuts on the width and length of shower images have long been used to perform background rejection in VHE astronomy, however a fixed width (or length) cut has a poor acceptance at high energy. To avoid this problem, cuts on a width (or length) parameter that scales with energy are needed. A method for accounting for the multiple telescope images is also needed. The HEGRA collaboration developed a parameter known as the mean-scaled-width (length) [8] for this purpose. In H.E.S.S., cuts on mean-reduced-scaled-width (MRSW) and length (MRSL) parameters are used. These parameters are defined as the mean of the difference in standard deviations for each telescope of the width (length) observed in the image from that which is expected from γ-ray simulations ($\langle$width$\rangle$ and σ) based on image intensity, reconstructed impact parameter and zenith angle (Z) of observations. The equation for MRSW is as follows:

$$MRSW = \frac{1}{N_{\rm tel}} \sum_{i=0}^{N_{\rm tel}} \frac{\rm width_i - \langle width_i \rangle}{\sigma_i} \, , \qquad (1)$$

and is similar for MRSL. The main difference from the HEGRA parameter, MSW = $1/N_{\rm tel} \sum_{i=0}^{N_{\rm tel}}$ width$_i$ / $\langle$width$\rangle_i$, is the incorporation of the standard deviation of the expected width. This accounts for the fact that the expected mean value may not be well determined for some values of the impact parameter and image intensity.

Figure 1 shows the distributions of MRSW for Monte Carlo (MC) γ-ray simulations, MC proton simulations, and off-source data. As required, the simulated proton and real cosmic ray (dominated by protons) distributions match well, illustrating that the response of H.E.S.S. is well simulated. The ability to remove the majority of background events while retaining a large fraction of γ-ray events is also clear. Figure 1 also shows the distribution of the observed excess from the Crab Nebula after all cuts are applied (excluding both the MRSW and MRSL cuts), as well as the corresponding distribution for MC γ-ray simulations, demonstrating that the simulations accurately characterize the detector response and that the detector performs as expected.

In addition to cuts on MRSW and MRSL, a cut on θ^2, the square of the angular difference between the reconstructed shower position and the source position, is ap-

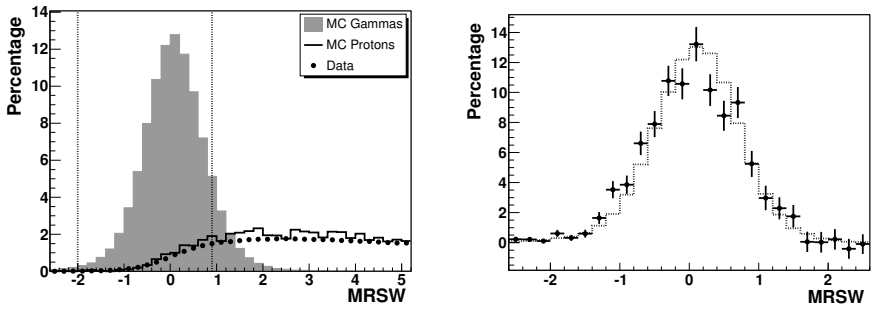

Figure 1: (Left) The distribution of MRSW for MC γ-ray simulations (photon index Γ=2.6), MC proton simulations, and off-source data, all at Z=20°. (Right) The distribution after cuts of MRSW (excluding both the shape cuts), for the background subtracted signal from observations of the Crab Nebula (points) and similarly for MC γ-ray simulations (Γ=2.6), both at Z=45°.

Cuts	MRSW max [σ]	Size min [PE]	θ^2 max [deg^2]	No θ^2 γ %	No θ^2 BG %	Q	All γ %	All BG %	Q
Std	0.9	80	0.0125	49	2.4	3.2	35	9.4e-3	36
Hard	0.7	200	0.01	15	0.23	3.2	13	7.5e-4	47
Loose	1.2	40	0.04	84	9.2	2.8	68	0.11	21

Table 1: The selection cuts applied to the data, the percentage of γ-ray (Γ=2.6, Z=20°) and background events (Z=20°) retained by those cuts, and the corresponding quality factors (Q) for analysis with and without the θ^2 cut. Cuts of MRSW$>$-2.0 and -2.0$<$MRSL$<$2.0 are applied in all cases.

plied in a point-source analysis[2], which is equivalent to placing the data into a round bin centered on the source position. All the cuts are optimized *a priori* to yield the maximum expected significance per hour of observation. The data used for optimization consist of MC γ-ray simulations at a zenith angle of 20° and real off-source data at comparable zenith angles. The optimal set of cuts depends heavily on the input spectrum used, however this is not known when searching for new sources of emission. In order to avoid having to correct for trials resulting from analysis with several sets of cuts or "over-optimizing" analysis of a given source, a set of standard cuts (optimized for a 10% Crab Nebula flux source with photon index Γ=2.6) were devel-

[2]For extended sources the θ^2 cut is replaced by an appropriate integration region.

oped. Although these cuts are used for all source analysis, a set of hard (optimized for a 1% Crab Nebula flux source with Γ=2.0) and loose (optimized for a Crab Nebula flux source with Γ=3.2) cuts were also generated. Use of the hard cuts results in a higher energy threshold, but events which pass them have a $\sim$20% better angular resolution and there are fewer systematic issues in estimating the remaining background. Therefore, the hard cuts are better suited for morphological studies of hard-spectrum sources. The loose cuts were designed for low-threshold spectral studies of bright sources, where the increased background (i.e. less significance) is not an issue. Table 1 shows the values of the cuts, the percentage of γ-rays and cosmic rays retained by the cuts, and their resulting quality factor.

2.3 Performance

Using MC simulations, the effective area of H.E.S.S. (after the various selection cuts) can be calculated and then convolved with a source energy spectrum to find the expected number of γ-rays detected versus energy. The peak of this distribution is commonly defined as the energy threshold of the detector. It should be noted that there are γ-ray photons detected below this energy. Figure 2 shows the energy threshold before and after the various selection cuts for a range of zenith angles (Z) calculated using the spectrum of the Crab Nebula as measured by HEGRA [9]. The energy threshold of H.E.S.S. at zenith is 100 GeV before selection cuts and remains below 1 TeV (after the standard selection cuts) for $Z<60^\circ$ within which almost all H.E.S.S. observations are performed. The increase in energy threshold after selection cuts is due to the minimum size cut applied to the data. Removing this cut lowers the post-selection energy threshold, but also lowers the expected significance from a source by $\sim$15% for the standard cuts.

The amount of observation time (live hours), at $Z=20^\circ$, required to detect a source for a range of fluxes ($>5\sigma$, assuming the HEGRA Crab Nebula spectrum) is calculated using the rate of simulated γ-rays passing selection cuts and the post-cuts rate of background events from actual off-source data, and shown in Figure 2. For comparison to the previous generation of instruments, HEGRA needed $\sim$100 hours to detect 5σ from a 5% Crab Nebula strength source, whereas H.E.S.S. only needs 1 hour of observations.

2.4 Energy Estimation

For each telescope image, the event energy is estimated using look-up tables containing the mean energy of simulated γ-rays in two-dimensional bins of image size and event impact parameter. The look-up tables are generated for 13 zenith angles ranging from 0° to 70° and an interpolation in cosine zenith angle (Z) is performed to return

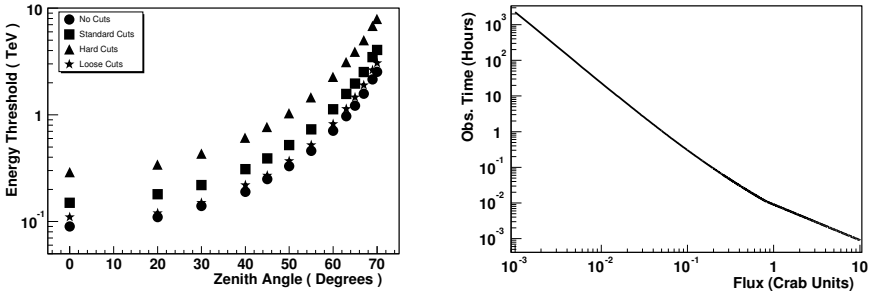

Figure 2: (Left) Energy threshold of H.E.S.S. before and after selection cuts *vs.* zenith angle. (Right) The observation time required to yield a 5σ detection at $Z{=}20^\circ$ *vs.* fraction of the Crab Nebula flux.

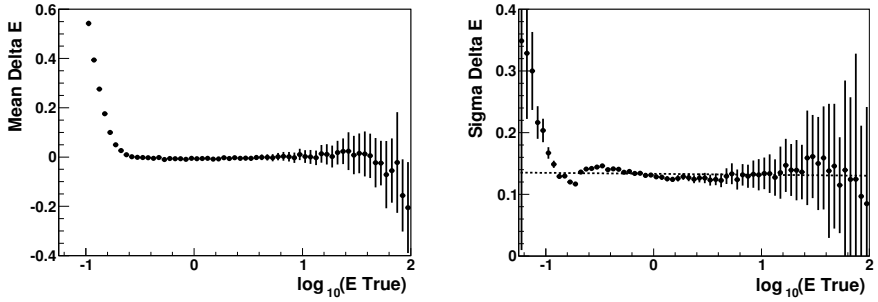

Figure 3: The mean (Left) and standard deviation (Right) of a Gaussian fit to the simulated γ-ray distribution of ($\mathrm{E_{fit}}$ - $\mathrm{E_{true}}$) / $\mathrm{E_{true}}$ for various bins of energy at a zenith angle of 20°.

the appropriate value. The energy of the observed γ-ray, $\mathrm{E_{fit}}$, is then calculated using the mean of the energies estimated for each telescope. Figure 3 shows the mean and standard deviation of a Gaussian fit to the simulated γ-ray distribution of "Delta E" = ($\mathrm{E_{fit}}$ - $\mathrm{E_{true}}$) / $\mathrm{E_{true}}$ for various bins of energy. The energy resolution of the instrument is commonly defined as this standard deviation. For all energies, this value is $\sim$15%.

2.5 Spectrum & Integral Flux Determination

In the determination of the energy spectrum, the data are logarithmically binned in energy. However, not all low-energy bins are used because the energy estimates for

events near the trigger threshold (i.e. at low energies) are on average too large (see Figure 3). Only bins for which the average bias in $\mathrm{E_{fit}}$ is less than 10% (approximately the post-selection-cuts energy threshold) are used to avoid any systematic effects. This effectively places a low-energy threshold (*safe threshold*) on suitable events. The range of bins used varies for each individual run due to the zenith angle of observation, and results in the bins at lower energies having differing amounts of exposure.

For each event passing cuts, the effective area, $\mathrm{A_{eff}}(\mathrm{E_{fit}},Z)$, is individually determined. The influence of the finite energy resolution has been taken into account in the effective areas, which are fit as a function of Z and $\mathrm{E_{fit}}$ for each of the various observation configurations similar to the method in [10]. Figure 4 shows the post-selection (standard) cuts effective area versus true and fit energy. As can be seen, there is little difference between the two curves, except at low energies due to the aforementioned bias. However, this low-energy region is avoided by the use of the *safe threshold*.

For each bin, the sum of $1/\mathrm{A_{eff}}$, is calculated for both on-source (O_i) and off-source (B_i) events using only events from the appropriate runs. Each bin in the spectrum then contains:

$$F_i = \frac{(O_i - B_i)}{\Delta E_i t_i} \, , \tag{2}$$

where t_i and ΔE_i are the exposure time and width in energy respectively for that bin. These data are then fit using an appropriate function (typically a power law).

It should be noted that the collection area as a function of fit energy depends on the spectral shape assumed because of the finite energy resolution. Figure 4 shows the ratio of the collection area calculated assuming various spectral shapes to that calculated assuming the initial spectral shape is flat in νF_ν (differential power-law index Γ=2.0) versus energy. For assumed spectra with Γ<3.0 the dependence is quite weak and can be ignored, but for softer spectra the effect can be important. Therefore, an iterative procedure is followed when determining the spectrum. First a flat (Γ=2.0) spectral shape is assumed. When deviations from this hypothesis are found the collection area is recalculated using the previous result and the spectrum is determined again. This procedure continues until convergence (typically 1-2 iterations). This spectral technique gives the input spectrum when a simulated signal, with real background, is tested. Additionally, the spectrum determined from H.E.S.S. observations of the Crab Nebula is in agreement with results from other instruments, and the spectra measured using the three aforementioned sets of cuts generally agree well. The systematic error on the photon index of a power-law fit to H.E.S.S. spectra is estimated to $\sim$0.1.

The observed integral flux from a source can be calculated with a simple integration of the observed spectrum above a given energy threshold. However, the observed excess from a source is often too small to generate an accurate spectrum on short time scales. In this case, a spectral shape is assumed (generally the time-averaged value from the source) and a flux calculated from the excess (Δ), the zenith angle (Z) expo-

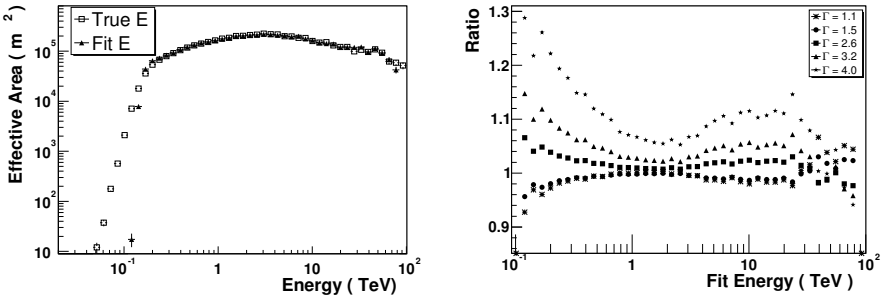

Figure 4: (Left) The post-selection (standard) cuts effective collecting of H.E.S.S. at 20° zenith angle *vs.* fit and true energy. (Right) The ratio of the post-selection (standard) cuts effective area calculated from simulations with different photon indicies to those with $\Gamma = 2.0$ *vs.* energy (Z=20°).

sure, t(Z), and the effective area ($\mathrm{A_{eff}}(E, Z)$) as a function of simulated (true) energy. The integral flux can then be calculated from the following equation:

$$\Delta = \int_{E_{min}}^{E_{max}} \int_{t_{start}}^{t_{stop}} \left(\frac{dN}{dE} \, \mathrm{A_{eff}}(E, Z(t)) \right) dt \, dE \, , \tag{3}$$

where dN/dE is the assumed spectrum. In the case of a power-law spectrum (dN/dE = I_o (E/TeV)$^{-\Gamma}$), Equation 3 is solved for I_o, and the integral flux (I) is calculated as I = $\int_{E_{min}}^{E_{max}} dN/dE \, dE$ = $\int_{E_{min}}^{E_{max}} I_o \, (E/\mathrm{TeV})^{-\Gamma} \, dE$. In the absence of a signal, upper limits are calculated by assuming a spectral shape and replacing Δ with a confidence value on the number of observed events. The systematic error on the integral flux (or upper limit) reported by H.E.S.S. is $\sim$20%.

3 Conclusions

The *Standard Analysis* is straightforward method for extracting signals and scientific results from H.E.S.S. observations. It has allowed the promised performance of the detector to be achieved, and has enabled the detection of more than 30 sources of VHE γ-rays. The results of the *Standard Analysis* agree well with those from other H.E.S.S. analysis techniques [2, 3], and this technique has the advantage of being quickly applied to any H.E.S.S. data set. This enables an "online" analysis, allowing observers in Namibia to know in less than one hour if a source has been detected.

References

[1] Hinton, J.A., 2004, *New Astronomy Reviews*, **48**, 331

[2] de Naurois, M., 2005, *these proceedings pp. 149-161*

[3] Lemoine-Goumard, M., 2005, *these proceedings pp. 173-181*

[4] Funk, S., *et al.*, 2004, *Astroparticle Physics*, **22**, 285

[5] Aharonian, F. *et al.*, 2004, *Astroparticle Physics*, **22**, 109

[6] Hillas, A.M., 1985, *Proceedings of the* 19^{th} *ICRC (La Jolla)*, **3**, 445

[7] Hoffman, W., *et al.*, 1999, *Astroparticle Physics*, **12**, 135

[8] Daum, A., *et al.*, 1997, *Astroparticle Physics*, **8**, 1

[9] Aharonian, F. *et al.*, 2000 *The Astrophysical Journal* **539**, 317

[10] Mohanty, G., *et al.*, 1998, *Astroparticle Physics*, **9**, 15